Acta Mech 223, 1169–1185 (2012)
DOI 10.1007/s00707-011-0609-5

Ali Pakniyat · Hassan Salarieh · Aria Alasty

Stability analysis of a new class of MEMS gyroscopes with parametric resonance

Received: 29 March 2011 / Revised: 25 November 2011 / Published online: 4 March 2012

Abstract In this paper, a parametrically resonated MEMS gyroscope is considered, and the effect of its parameters on the system stability is studied. Unlike the general case of MEMS gyroscopes with harmonic excitation, in this new class of gyroscopes with parametric excitation, the origin is one stationary point of the system. The study starts with the stability analysis of the origin, and then it goes on to analyze the effect of each parameter on the stability of periodic orbits. Stabilities are studied by means of Floquet theory. As the results indicate, presence of a non-trivial response for the system is closely interconnected to the stabilities (and instabilities) of the system. It is demonstrated that the stability of the origin always contributes to a zero response for the sensor, and hence the instability of origin is required for the occurrence of parametric resonance. In contrast, stability of a periodic orbit does not necessarily guarantee a resonant response for the gyroscope, and again it is the instability of the origin which is required for this purpose. Because in the case of linear stiffness—linear parametric excitation the instability of the origin results in instability of the system, it is concluded that nonlinearities are required for a parametrically actuated gyroscope.

1 Introduction

Gyroscopes can be classified into three categories: rotating, optic, and vibrating gyroscopes. The first two kinds are too heavy and too large to be used broadly in many applications. However, the vibrating-type MEMS gyroscopes are smaller, lighter, and cheaper. They need less power, have higher reliability, and can be multifunctional. These devices are so small that they can be integrated with the electronic circuits required for their operation.

Various types have been proposed and used for MEMS gyroscopes. For instance, tuning forks, ring-type, cantilever-type, and lumped mass gyroscopes are some examples of these types. In all of the vibrating gyroscopes, there is an actuation force which causes part of the sensor to vibrate in one direction called the drive mode. The vibrating part of the gyroscope also has some other degrees of freedom in one or more directions called the sense mode(s), which is ideally decoupled from the drive mode in the absence of external rotation rate. In the presence of an external rotation speed, the sense mode becomes coupled to the drive mode as a result of the produced Coriolis force.

In order to obtain high amplitudes in the drive mode by consumption of minimal energy, the drive mode should be resonated by the excitation voltage. Furthermore, to have a more accurate reading for the sensor (i.e., high amplitudes in this mode), the signal in the drive mode should provide resonance in the sense mode.

A. Pakniyat · H. Salarieh (✉) · A. Alasty
Center of Excellence in Design, Robotics and Automation (CEDRA), School of Mechanical Engineering,
Sharif University of Technology, PO Box 11155-9567, Tehran, Iran
E-mail: salarieh@sharif.edu
Tel.: +98-21-66165538
Fax: +98-21-66000021

In almost all of the currently fabricated gyroscopes, the actuation mechanism is a simple harmonic voltage and hence, to meet the aforementioned requirements, the resonant frequencies in both modes should be matched [1]. However, the requirement of matched modes is hard to provide due to unavoidable imperfections in the manufacturing process. As a result, most designs are not based on matched vibration mode frequencies [1] and therefore do not provide high amplitudes in the output of the sensor.

To overcome the problem of mode mismatching, a number of methods have been proposed and put into practice. These methods can be categorized into three distinct groups. Since the mismatching is due to the manufacturing process (i.e., difference in stiffness of the two modes), the first group concentrates on the fabrication process in order to provide equal restoring forces in the two directions. For instance, Liu et al. [2] presented a new design for the spring beams and optimized the shape of the suspension beams by a cellular automata approach, and Alper et al. [3–5] proposed a structure for a suspension system that provides decoupled and adjustable stiffness in the two modes. The adjustment is performed using an extra set of comb fingers which electrostatically alter the natural frequencies. The method proposed by Jeong et al. [6] is also based on electrostatic tuning of stiffness.

Since post-manufacturing techniques require manual tunings, they are not suitable for mass production [7] and hence, the second group tries to implement closed loop control techniques to match the modes. For instance, Sung et al. [7–9] provided resonance in both modes through phase-locked loop (PLL) control, and Park et al. [10–13] used adaptive force control for this purpose.

While the first two categories increase the cost of the sensor because of extra manufacturing processes or additional devices for control purposes, the third group utilizes parametric resonance which is not based on mode matching. The idea of employing parametric resonance was first proposed by Oropeza-Ramos et al. [14]. Since parametric excitation can be applied only by replacement of interdigitated comb fingers by non-interdigitated ones [14–19], parametric resonance does not impose extra financial burden on the fabrication of the gyroscope. In addition, parametric resonance is robust to parameter changes and hence, such a gyroscope does not require post-manufacturing tunings.

The idea of implementing parametric excitation for MEMS gyroscopes (instead of the common method of harmonic excitation) was studied through a frequency analysis by Miller et al. [20] for the purpose of predicting the occurrence of parametric resonance. Based on this study and some experimental evaluations, a gyroscope was arranged to work based on this phenomenon [15–17].

However, the study performed by the present authors [21] pointed out that the frequency approach, although is suitable for providing parametric resonance in the drive mode, does not necessarily guarantee the occurrence of resonance in the sense mode. A parametric study on the system indicates that there are some sets of parameters for which the output of the sensor is amplified significantly higher than what has been previously reported by Oropeza-Ramos et al. [14–19]. This parametric study is beyond the scope of this paper which studies the stability of such a parametrically excited gyroscope with the parameters having the values presented in Table 2. For more information, one can refer to [21] or follow the future publications of the authors.

When parametric excitation is used, the dynamic characteristics of the gyroscope change significantly. For instance, the time-invariant governing equation of a harmonically excited gyroscope becomes time-varying when parametric excitation is used. Furthermore, zero response (trivial solution) is always one possible response for a parametrically excited gyroscope even in the presence of nonzero excitation (hence instability of the origin would be desirable), while a harmonically excited gyro would never have zero response in presence of nonzero excitation. But the most important change provided by parametric excitation is that parametric resonance occurs in a wide range of frequencies, while harmonic resonance only takes place at the vicinity of one specific frequency (the natural frequency). This last property provides robustness to manufacturing imperfections.

In the previous study [22], the stability of the origin for the system designed by Oropeza-Ramos et al. [14–17] was studied, and it was shown that the origin was exponentially stable for the considered system. To overcome the problems associated with the stability of the origin, it was suggested to add a harmonic term to the parametric excitation to make the origin not be a stationary point of the system [22]. A parametric study on the system [21] indicated that there are other sets of parameters that can provide much higher amplitudes for the sensor. In this paper, the previous study [22] is extended to analyze the stability of both the origin and periodic orbits of a parametrically excited MEMS gyroscope, and it is shown that the stability-related problems for the gyroscope designed by Oropeza-Ramos et al. [14–17] do not exist for the system with new suggested values of parameters. In addition, the stability of the origin is studied for different values of the system parameters, and it is shown that instability of the origin is related to the occurrence of parametric resonance. After that, the effect of each parameter on the stability of the periodic orbit is analyzed.

2 Statement of the model

In this paper, a gyroscope with a single lumped mass is considered. The simplified equivalent structure of the device is shown in Fig. 1.

Considering pure rotation of the gyroscope's frame about the z-axis, the equation of motion for the system shown in Fig. 1 is presented in Eq. (1), where m is the mass, F^d is damping force, F^r represents the elastic restoring forces provided by the springs, and $F^a\ (x,t)$ corresponds to the parametric actuation force. Note that the terms $2m\Omega_z\dot{y}$ and $-2m\Omega_z\dot{x}$ represent the rotation-induced Coriolis forces, and the terms $mx\Omega_z^2$ and $my\Omega_z^2$ are related to the centripetal acceleration required for rotation of the mass about the z-axis,

$$\begin{aligned} m\ddot{x} + F_x^d + F_x^r &= F^a\,(x,t) + 2m\Omega_z\dot{y} + mx\Omega_z^2, \\ m\ddot{y} + F_y^d + F_y^r &= -2m\Omega_z\dot{x} + my\Omega_z^2. \end{aligned} \tag{1}$$

The damping and restoring forces are considered to behave as in Eq. (2):

$$\begin{aligned} F_x^d &= c\dot{x}, & F_y^d &= c\dot{y}, \\ F_x^r &= k_1x + k_3x^3, & F_y^r &= k_1y + k_3y^3. \end{aligned} \tag{2}$$

In order to generate a parametric excitation, the actuation force is produced by a set of non-interdigitated comb fingers with the equation described by:

$$F^a\,(x,t) = -\left(r_1x + r_3x^3\right) V\,(t)^2\,. \tag{3}$$

In Eq. (3), r_1 and r_3 are electrostatic coefficients that depend on the physical dimensions and spacing of the electrostatic comb drives, and $V(t)$ is the voltage applied across the drives [14–16]. Since the electrostatic force has a square dependence on the applied voltage, it is proposed to use a square-rooted sinusoidal signal as in Eq. (4) in order to isolate the parametric effects from the harmonic response [14–16],

$$V\,(t) = V_A\,(1 + \cos\,(\omega t))^{1/2}\,. \tag{4}$$

Substituting F^a and F^r in Eq. (1) and re-scaling the parameters, the gyroscopic system is described by

$$\begin{aligned} x'' + \alpha x' + (\delta_{x1} + 2\beta_1\cos 2\tau)\,x\, + (\delta_{x3} + 2\beta_3\cos 2\tau)\,x^3 - \gamma y' &= 0, \\ y'' + \alpha y' + \delta_{y1}y + \delta_{y3}y^3 + \gamma x' &= 0. \end{aligned} \tag{5}$$

The derivative operator and the scaled parameters used in Eq. (5) are defined in Table 1.

Note that the two parameters δ_{x1} and δ_{x3} are not independent from other parameters because by the definition of the parameters in Table 1, the equalities $\delta_{x1} = \delta_{y1} + 2\beta_1$ and $\delta_{x3} = \delta_{y3} + 2\beta_3$ must be held. The method for finding the parameter values that correspond to high-amplitude parametric resonance in the gyroscope is

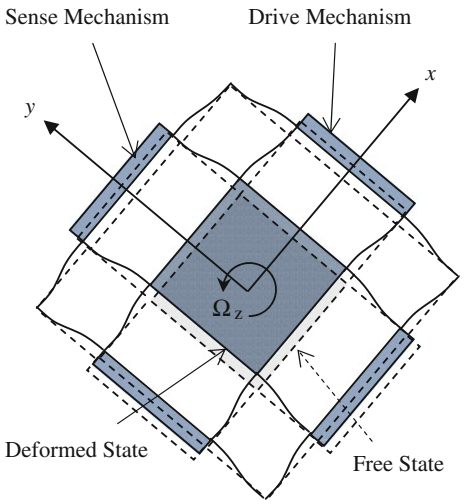

Fig. 1 Structure of the MEMS gyroscope considered in this paper

Table 1 The derivative operator and the scaled parameters

$\alpha = \frac{2c}{m\omega}$	$\gamma = \frac{4\Omega_z}{\omega}$
$\beta_1 = \frac{2r_1 V_A^2}{m\omega^2}$	$\beta_3 = \frac{2r_3 V_A^2}{m\omega^2}$
$\delta_{x1} = \frac{4k_1}{m\omega^2} + 2\beta_1 - \frac{\gamma^2}{4}$	$\delta_{y1} = \frac{4k_1}{m\omega^2} - \frac{\gamma^2}{4}$
$\delta_{x3} = \frac{4k_3}{m\omega^2} + 2\beta_3$	$\delta_{y3} = \frac{4k_3}{m\omega^2}$
$2\tau = \omega t$	$(.)' = \frac{d(.)}{d\tau}$

Table 2 Three sets of parameters values for obtaining resonant high amplitudes for the gyroscope

	Set 1	Set 2	Set 3
δ_{y1}	1	1	4
β_1	4.2	13.5	6.5
β_3	0	0	0
α	0.01	0.01	0.01
γ	0.001	0.001	0.001

beyond the scope of this paper. We just consider the values found from a parametric study on design of the gyroscope [21] and study the effect of variations of each parameter around the resonating values presented in Table 2. It should also be mentioned that the parameter δ_{y3} has only a scaling effect on the output of the sensor, and hence the assumption $\delta_{y3} = 1$ can be made without loss of generality.

Ruling out the nonlinear terms in Eq. (5) by setting δ_{y3} and β_3 (corresponding to k_3 and r_3) equal to zero, the equation of motion for the linear system corresponding to the nonlinear system in Eq. (5) is presented by Eq. (6),

$$\begin{aligned} &x'' + \alpha x' + (\delta_{x1} + 2\beta_1 \cos 2\tau)\, x - \gamma y' = 0, \\ &y'' + \alpha y' + \delta_{y1} y + \gamma x' = 0. \end{aligned} \tag{6}$$

Notice that unlike harmonic excitation for which there is no equilibrium point in the presence of a nonzero actuation and hence the system has always a periodic response, for parametric excitation as given by Eqs. (5) and (6), the origin (or zero state) is always one stationary point of the system. As a result, there may or may not exist a nonzero periodic response for a parametrically excited system. In this paper, by studying the stability of both the origin and the periodic response, the relationship between these stabilities and occurrence of parametric resonance is explained. To this end, it is first shown that the linear system in Eq. (6) has no asymptotically stable periodic orbit other than zero. After that, the stability of the nonlinear system in Eq. (5) is studied in two parts. First, the stability of the origin for Eq. (5) is discussed based on the stability of Eq. (6); then, the relationship between the instability of the origin and occurrence of parametric resonance is presented. After that, stability of the periodic orbits of Eq. (6) will be examined, and the effect of each parameter on this stability will be discussed.

In this paper, Floquet theory is employed for the purpose of stability analysis. In the following Section, the reasons that Floquet theory was selected for this purpose are discussed.

3 Stability criterion

Although the most common stability criterion in the analysis of nonlinear systems is the Lyapunov theorem, for the following reasons it is not appropriate for the present purpose which is the analysis of the stability of both the origin and the periodic orbits of the considered gyroscope:

(i) Lyapunov criterion is designated for verification of stability of the equilibrium point (the origin, in this problem). When the stability of periodic orbits is desired, it is required to have the analytical equation of the orbit to subtract from the main equation, which is not available in many cases (including the considered gyroscope), and even when available, the resulting equation is typically more complicated than the system itself.

(ii) Lyapunov criterion is a sufficient condition for stability and is not a necessary condition. In addition, Lyapunov-based instability criteria are also sufficient conditions, and as a consequence, there might be regions for which neither stability nor instability can be proved.
(iii) Lyapunov does not provide a quantitative measure for stability, and it cannot be used to study the effect of changing parameters on the stability behavior. In addition, when parameters of the system are changed, sometimes the Lyapunov function is required to be changed so that stability can be proved.
(iv) Lyapunov criterion is rather more complex for non-autonomous systems (including the considered gyroscope).

In contrast, since the governing equations of the considered gyroscope are periodic, based on the following reasons, Floquet theory would be a suitable tool for stability analysis of the considered system:

(i) Floquet theory is explicitly developed for the analysis of periodic orbits of a periodic system. In this paper, it will be shown how this tool can be extended to examine the stability of the origin for the considered gyroscope.
(ii) Stability and instability are examined simultaneously when using Floquet theory. As a result, boundaries between stability and instability can be determined precisely.
(iii) It provides a quantitative measure of stability, and hence it can easily be applied to study the effect of changing a particular parameter on the stability characteristics of the system.
(iv) Since it is a numerical tool, it is as simple for non-autonomous systems as it is for autonomous ones.

In the next section, Floquet theory is introduced briefly.

4 Floquet theory

Consider the general set of inhomogeneous, non-autonomous differential equations (7):

$$\dot{x} = F(x,t) = F(x,t+T) \quad \text{where} \quad F(0,t) \neq 0. \tag{7}$$

Assume that this set of differential equations has a periodic solution $x_r(t) = x_r(t+T)$. For a sufficiently small perturbation $\tilde{x}(t)$ (such that $x(t) = x_r(t) + \tilde{x}(t)$), the linearized dynamics of the perturbation term will be of the form of Eq. (8)

$$\dot{\tilde{x}}(t) = D(t)\,\tilde{x}(t) \tag{8}$$

where

$$D(t) = \left.\frac{\partial F(x,t)}{\partial x}\right|_{\tilde{x}(t)=0} = \left.\frac{\partial F(x,t)}{\partial x}\right|_{x(t)=x_r(t)}. \tag{9}$$

The periodic solution of Eq. (7) is stable (i.e., the influence of perturbation $\tilde{x}(t)$ will fade away) if and only if the magnitudes of all the eigenvalues of the so-called monodromy matrix are less than unity. Monodromy matrix is defined as the solution of the set of differential equations (10) for the state transition matrix $\Phi(t)$ with the initial condition of $\Phi(0) = I$ evaluated at the time T as in Eq. (11).

$$\dot{\Phi}(t) = D(t)\,\Phi(t), \tag{10}$$

$$M = \Phi(T). \tag{11}$$

Each eigenvalue of the monodromy matrix M is referred to as a *Floquet Multiplier* (or *Floquet Exponent*) of the system and is a measure of the fading rate of the perturbation in the direction of the corresponding eigenvector. When the magnitudes of all Floquet multipliers are less than unity, the perturbation has faded away in each direction after one period T. Because of the periodic nature of Eq. (7) which means that the same transformation matrix M operates at every revolution (period), it can be concluded that the perturbation $\tilde{x}(t)$ will finally approach the zero state.

If only one of the Floquet multipliers has a magnitude larger than unity, the perturbation will grow exponentially in that direction and consequently $x_r(t)$, the periodic solution of the system, is unstable. For the case when the magnitude of one of the Floquet exponents is unity (while others have a magnitude less than 1) Floquet theory cannot conclude stability or instability because of the linearization. In this case, stability should be determined through extra techniques.

Now we go back to our system in Eqs. (5) and (6). First, in the following Section, stability of the linear system (6) is studied and after that, stability of the nonlinear system (5) is examined based on the stability results of the linear system.

5 Stability of the linear system

In this Section, it is shown that when the values of the nonlinear terms in Eq. (5) are small so that they can be neglected, the corresponding linear system in Eq. (6) can never possess any asymptotically stable periodic solution other than zero. When stability conditions predict an asymptotic stable periodic response for the linear system in Eq. (6) (i.e., when the Floquet multipliers are less than unity), this response would be the trivial solution. The important outcome of this Section is that it shows how exponential stability of the origin can be concluded from Floquet exponents of the linear system. This is shown in Proposition 1.

Proposition 1 *The system in Eq. (6) has no asymptotically stable periodic response other than trivial solution. Furthermore, if the asymptotic stability is obtained from the magnitude of the Floquet exponents*[1] *lying below 1, the origin is globally exponentially stable.*

Proof of Proposition 1 By defining the state variables as $x_1 = x\ ,\ x_2 = x'\ ,\ x_3 = y\ ,\ x_4 = y'$, the system in Eq. (6) can be rewritten in the form of Eq. (12)

$$\begin{bmatrix} x_1' \\ x_2' \\ x_3' \\ x_4' \end{bmatrix} = \begin{bmatrix} 0 & 1 & 0 & 0 \\ -(\delta_x + 2\beta_x \cos 2\tau) & -\alpha_x & 0 & \gamma \\ 0 & 0 & 0 & 1 \\ 0 & -\gamma & -\delta_y & -\alpha_y \end{bmatrix} \begin{bmatrix} x_1 \\ x_2 \\ x_3 \\ x_4 \end{bmatrix} \quad or \quad \underline{x}' = A(\tau)\underline{x}. \tag{12}$$

Because the system is linear, the dynamics of the perturbation term will be in the form of Eq. (12), that is, the same as the dynamics of the system itself,

$$\underline{\tilde{x}}' = D(\tau)\underline{\tilde{x}} = \left.\frac{\partial F}{\partial x}\right|_{x=x_r} \underline{\tilde{x}} = A(\tau)\underline{\tilde{x}}. \tag{13}$$

Now assume that there is an asymptotically stable periodic solution for Eq. (6). The asymptotic stability of this periodic orbit requires asymptotic stability of the origin for the perturbation term (Eq. (13)) which is equivalent to asymptotic stability of the origin for Eq. (12). But for a linear system, the stability is global meaning that for every initial condition the response would asymptotically reach the zero state. Hence, the linear system has no asymptotically stable periodic response other than the trivial solution.

To prove the exponential stability of the origin which is required later in the Sect. 6.1, we should note that asymptotic stability through Floquet multipliers requires that $\forall i: \quad |\lambda_i| < 1$. Denoting $\max\left\{\left|\lambda_i(M^T M)\right|^{1/2}\right\}$ by ρ, we can write

$$\|x(t+T)\| = \|\Phi(T)\, x(t)\| \leq \rho \|x(t)\|. \tag{14}$$

Because of the periodic nature of the governing equations, it can be shown that (see [23]):

$$\Phi(kT) = \Phi^k(T) \tag{15}$$

and also

$$\lambda(\Phi(kT)) = \lambda\left(\Phi^k(T)\right) = \lambda^k(\Phi(T)). \tag{16}$$

So, we may write:

$$\|x(t+nT)\| \leq \rho^n \|x(t)\| = e^{n\ln\rho} \|x(t)\|. \tag{17}$$

By defining $\mu \stackrel{\Delta}{=} -\ln\rho$ and remembering that $0 < \rho < 1 \quad \Rightarrow \quad \mu > 0$, we can write:

$$\|x(t+nT)\| \leq e^{-n\mu} \|x(t)\|. \tag{18}$$

This equation illustrates the exponential stability of the origin. Due to the linear nature of Eqs. (6) and (12), this holds for any initial condition in $\mathbb{R}^2$ and hence, stability and instability properties of the origin are global.

[1] Defined as the singular values of the monodromy matrix.

Establishing conclusions of the origin stability based on Floquet exponents can be explained as follows: Since in the stability analysis of periodic orbits for the linear system (12) the equation of the orbit itself does not appear, the stability of all possible orbits would be computed the same. Because the trivial solution is a periodic response with any assumed period including the period of excitation, when Floquet exponents are computed, the stability of the origin is determined. As a conclusion, if there would be any asymptotically stable periodic orbit, the origin is globally exponentially stable for Eq. (12) and hence, all responses will move toward the origin starting from any possible initial condition. As a result, the only possible asymptotically stable periodic response for the system (12) is the trivial solution. Note that without Proposition 1, the period T required for the computation of Floquet exponents for stability of the origin cannot be provided.

6 Stability analysis of the nonlinear system

The state space equation of the nonlinear system (5) is presented in Eq. (19):

$$x' = F(x,\tau) = \begin{Bmatrix} x_2 \\ -\alpha_x x_2 - (\delta_x + 2\beta_x \cos 2\tau)\, x_1 - (\delta_{x3} + 2\beta_{x3} \cos 2\tau)\, x_1^3 + \gamma x_4 \\ x_4 \\ -\alpha_y x_4 - \delta_y x_3 - \delta_{y3} x_3^3 - \gamma x_2 \end{Bmatrix}. \tag{19}$$

In this Section, stabilities related to this nonlinear system including the stability of the origin and the stability of the periodic orbits are studied. The importance of the stability of the origin is that when it is stable, for the initial states within the region of attraction of the origin, the steady output of the gyroscope is zero which is not acceptable for the sensor. In contrast, when the origin becomes unstable, responses of the system escape from the rest condition and reach the existing stable periodic orbits.

In the following, Sect. 6.1 concerns the stability of the origin for the nonlinear system (19), and Sect. 6.2 discusses the stability of periodic orbits of Eq. (19).

6.1 Stability of the origin for the nonlinear system

In this Section, stability of the origin for the nonlinear system (19) is verified based on the stability of the linear system (12), and it is shown that the origin is either unstable or exponentially stable[2] for Eq. (19). To this end, we first introduce a theorem that relates the stability of the origin for a nonlinear system to the stability of the origin for its corresponding linear system, and then in Proposition 2, we show that the origin stability for Eq. (19) can be verified based on the Floquet exponents of Eq. (12).

Theorem[3]

Let $x = 0$ be an equilibrium point for the nonlinear system

$$\dot{x} = F(x,t) \tag{20}$$

where $F : [0,\infty) \times D \to \mathbb{R}^n$ is continuously differentiable, $D = \{x \in \mathbb{R}^n \text{ such that } \|x\|_2 < r\}$, and the Jacobian matrix $[\partial F/\partial x]$ is bounded and Lipschitz on D uniformly in t. Also let

$$A(t) = \left.\frac{\partial F(x,t)}{\partial x}\right|_{x=0}. \tag{21}$$

Then, the origin is an exponentially stable equilibrium point for the nonlinear system (19) if it is an exponentially stable equilibrium point for the linear system in (22):

$$\dot{x} = A(t)\, x. \tag{22}$$

The region of attraction for Eq. (20) contains Ω_ρ where $\Omega_\rho = \{\|x\|_2 \le \rho\}$ for some $0 < \rho \le r$.

[2] Since the case of maximum Floquet exponent equal to 1 happens only in stability boundaries, this case is not concerned separately, and it is regarded as a transition from stability to instability.

[3] To find this theorem and its proof, see [24].

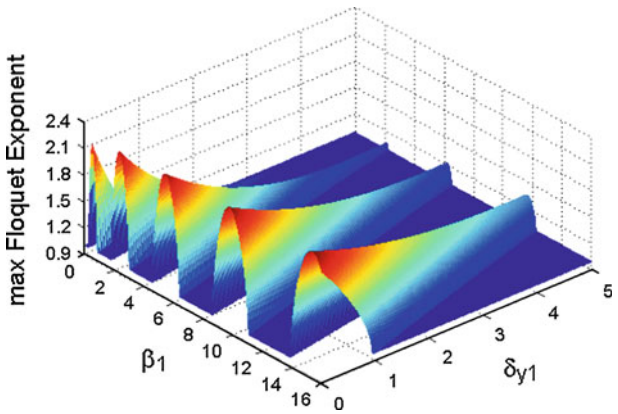

Fig. 2 Stability of the origin for the considered gyroscope based on max Floquet exponent of the linear system for different values of δ_{y1} and β_1

Proposition 2 *Stability of the origin for the parametrically excited gyroscope in Eq.* (19) *can be verified from the Floquet exponents of the corresponding linear system* (12)*. In the case of asymptotic stability of the origin, the zero state is exponentially stable with non-empty basin of attraction containing the origin.*

Proof of Proposition 2 Since the zero response satisfies Eq. (19), the origin is an equilibrium point for the equation $x' = F(x, \tau)$. Also, it can be easily shown that F is continuously differentiable. The Jacobian matrix is computed as:

$$\frac{\partial F}{\partial x} = \begin{bmatrix} 0 & 1 & 0 & 0 \\ \begin{pmatrix} -(\delta_x + 2\beta_x \cos 2\tau) \\ -3(\delta_{x3} + 2\beta_{x3} \cos 2\tau) x_1^2 \end{pmatrix} & -\alpha_x & 0 & \gamma \\ 0 & 0 & 0 & 1 \\ 0 & -\gamma & -\delta_y - 3\delta_{y3} x_3^2 & -\alpha_y \end{bmatrix}. \tag{23}$$

The Jacobian matrix in Eq. (23) and its derivative with respect to x (which is a 3-dimensional matrix with $4 \times 4 \times 4$ dimension) are bounded in any bounded region $[0, \infty) \times D$ where $D = \{x \in \mathbb{R}^n \ such\ that\ \|x\|_2 < r\}$. So $[\partial F / \partial x]$ is Lipschitz on D. Because $\cos 2\tau$ is bounded, this Lipschitz property is uniform in τ. Moreover, the linear system corresponding to Eq. (19) is derived in Eq. (24) which contributes to the same equation as the equation of the linear system (12) for which the exponential stability of the origin was determined,

$$A(\tau) = \left.\frac{\partial F(x, \tau)}{\partial x}\right|_{x=0} = \begin{bmatrix} 0 & 1 & 0 & 0 \\ -(\delta_x + 2\beta_x \cos 2\tau) & -\alpha_x & 0 & \gamma \\ 0 & 0 & 0 & 1 \\ 0 & -\gamma & -\delta_y & -\alpha_y \end{bmatrix}. \tag{24}$$

Since all the requirements in the mentioned Theorem are satisfied, the condition of Floquet exponents of Eq. (19) being less than unity verifies local exponential stability of the origin with some region of attraction Ω containing Ω_ρ.

Now that the tool for analyzing the stability of the origin has been developed, stability or instability of the origin for different parameters values is studied. According to Proposition 2, nonlinear terms have no effect on the stability of the origin for the nonlinear system since this stability is determined exclusively from the linear system. It should be noted that when one Floquet exponent has a magnitude equal to 1, and hence stability of the origin cannot be concluded from Proposition 2, nonlinear terms may contribute to either the origin stability or its instability. However, according to the results (see Fig. 2 through 7), for the considered gyroscope, the case of maximum Floquet exponent equal to unity occurs only on a boundary line and not a surface region and so, this case coincides with marginal stability. In conclusion, the only terms that can influence the stability of the origin are δ_{x1}, δ_{y1}, β_1, α, and γ. However, since the equality $\delta_{x1} = \delta_{y1} + 2\beta_1$ holds (see Table 1), there are only four independent parameters δ_{y1}, β_1, α and γ that influence stability of the origin.

Since the most important factors for occurrence of resonance in the system are δ_{y1} and β_1, the nominal values for α and γ are considered to be 0.01 and 0.001, respectively, as in Table 2, and the maximum magnitude

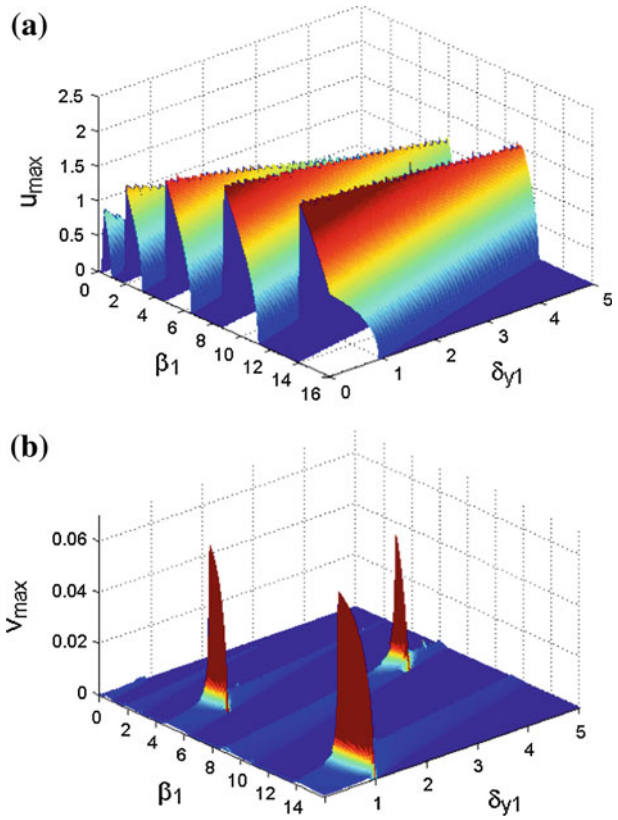

Fig. 3 Maximum steady state amplitude in **a** drive mode and **b** sense mode for different values of δ_{y1} and β_1

of Floquet exponents for different values of δ_{y1} and β_1 is studied in Fig. 2. In this Figure, for some values of δ_{y1} and β_1, the maximum magnitude of Floquet exponents is less than 1 (the plate in the floor of the figure with max Floquet exponent around 0.98), which based on Proposition 2 shows exponential stability of the origin. For other sets of values, the maximum Floquet exponent lies above the z = 1 plane[4], which shows instability of the origin.

Comparing the stability of the origin (Fig. 2) with the maximum amplitudes in the two modes (Fig. 3 [22]), it is demonstrated how the instability of the origin contributes to parametric resonance in the system. In all regions for which the origin is stable (i.e., the maximum magnitude for the Floquet exponents lies below the z = 1 plane), the maximum amplitude in both modes is zero (see Fig. 3). In contrast, whenever the maximum magnitude of the Floquet exponents is above 1, parametric resonance occurs in drive mode (Fig. 3a) and furthermore, the amplitude in the sense mode (Fig. 3b) becomes nonzero. However, resonant amplitudes in the sense mode require more conditions than instability of the origin. For resonance to occur in the sense mode, the produced signal in the drive mode should contain enough frequency content of the sense mode natural frequency. In the studied region, this occurs only for $\delta_{y1} = 1$ and $\delta_{y1} = 4$ for some resonance regions corresponding to β_1 (see Fig. 3b and also Table 2).

By considering $\delta_{y1} = 1$, for different values of β_1 and α, the stability characteristic of the origin is presented in Fig. 4. For $\delta_{y1} = 4$, the behavior is the same and hence is not illustrated here.

As was expected from the relationship of the maximum Floquet exponent with the term β_1 (at the cross section $\delta_{y1} = 1$ of Fig. 2), the same regions of β_1 for which a change in the maximum Floquet exponent occurs do not vary for different values of α. However, in both resonating and non-resonating values of β_1, the maximum Floquet exponent decreases by increasing α, which demonstrates that the stability of the origin is increased. This means that for larger values of α, parametric resonance occurs with increased difficulty. To illustrate this point, instability regions of Fig. 4 are presented in Fig. 5.

[4] Here, z is the vertical axis corresponding to maximum Floquet exponent.

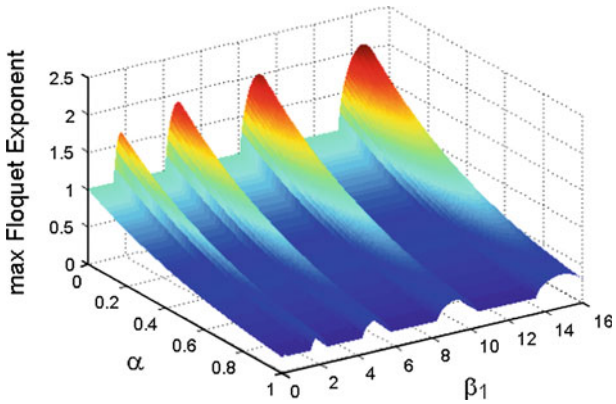

Fig. 4 Stability of the origin for the considered gyroscope based on max Floquet exponent of the linear system for different values of β_1 and α

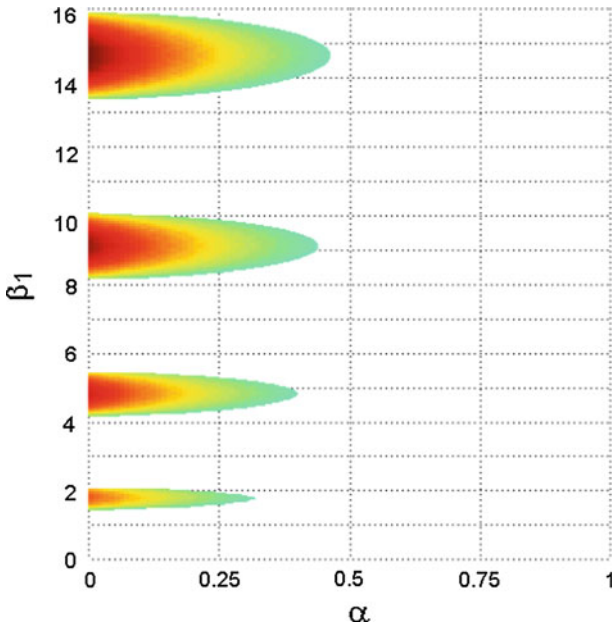

Fig. 5 Regions of instability of the origin for different values of β_1 and α

The colored regions in Fig. 4 are the regions for which the magnitude of at least one Floquet exponent is larger than unity, and consequently the response of the gyroscope escapes from the rest condition and moves toward probably periodic orbits. A full study on the existence and stability of periodic orbits in this case is beyond the scope of this paper. It is just mentioned that although for different values of β_3 bifurcations in the system change the stability and the number of periodic orbits, for $\beta_3 = 0$ and the values near zero, there are always stable resonant periodic orbits with regions of attraction containing the origin. Therefore, when the origin becomes unstable, the response of the gyroscope moves toward a stable periodic orbit.

Comparison of Fig. 4 (and Fig. 5) at the cross section $\beta_1 = 4.2$ with Fig. 6 shows again the relationship between instability of the origin and resonance in both modes. Note that for $\delta_{y1} = 1$ and $\beta_1 = 4.2$, both modes are in resonant conditions. It is interesting to note that Fig. 6 shows that the strength of instability of the origin does not have a significant influence on the resonant amplitudes in the drive mode, but the vibration amplitude of the sense mode is affected significantly by damping. However, it would be incorrect to assume that this decrease in amplitude in the sense mode is due to the decrease in maximum Floquet exponent since an examination on the corresponding direction of the maximum eigenvalue demonstrates that the eigenvalues corresponding to the eigenvectors in the direction of the sense mode are less than 1. In fact, in the resonating regions, it is the drive mode whose corresponding Floquet exponents become more than 1, resulting in the

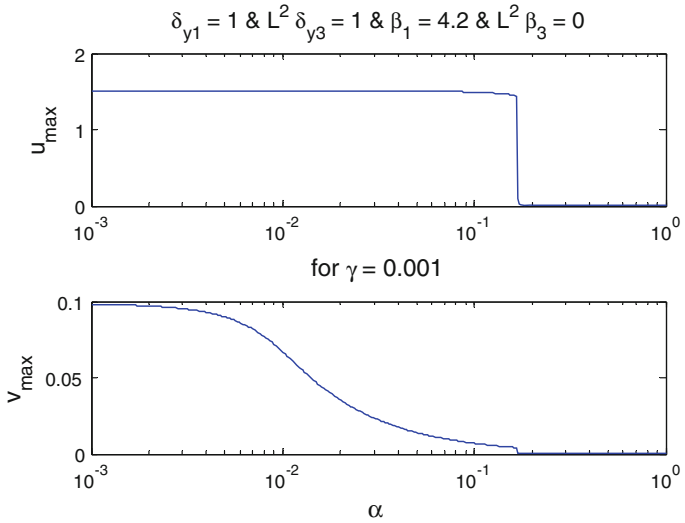

Fig. 6 Steady state amplitude in drive mode (*top*) and sense mode (*bottom*) for different values of α

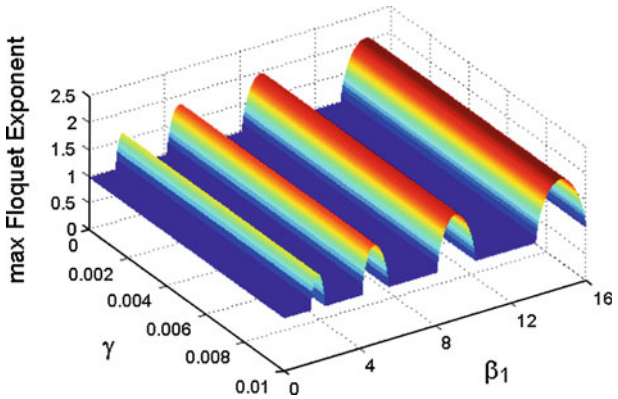

Fig. 7 Stability of origin for the considered gyroscope based on max Floquet exponent of the linear system for different values of β_1 and γ

instability of the origin. The main reason for the noted decline in the sense mode amplitude is the reduction of another Floquet exponent with a magnitude less than 1.

Comparison of Figs. 5 and 6 also shows how stability of the origin results in a decrease in resonant amplitudes for the gyroscope. Around $\alpha = 0.178$, the maximum magnitude of the Floquet exponents falls below 1 and the origin becomes exponentially stable with a non-empty region of attraction (see Proposition 2). As a result, the system response is absorbed by the origin, which is explaining why amplitudes in both modes become zero in the right side of Fig. 6.

According to performance issues, γ should be kept below 0.01 in order to prevent a significant change in δ_{y1} (see Table 1). In Fig. 7, the effect of γ in the region $\gamma < 0.01$ is studied. This figure shows that in both resonant and non-resonant regions (based on the value of β_1), γ has no effect on the stability of the origin for a parametrically resonated MEMS gyroscope. Note that large γ makes the operation of the sensor unstable, but these values are out of the operational range of the gyroscope and hence are not considered here.

In addition to the information provided by the maximum magnitude of the Floquet exponents, further properties of the system can be obtained from the product of all Floquet exponents. Note that since the Monodromy matrix is a real square matrix, Floquet exponents are either real or in complex conjugate pairs and as a consequence, the product of Floquet exponents is a real value. This value is a measure of expansion or contraction of the response of the perturbation term, which, based on Proposition 2, will show the behavior of the response of the system near the origin.

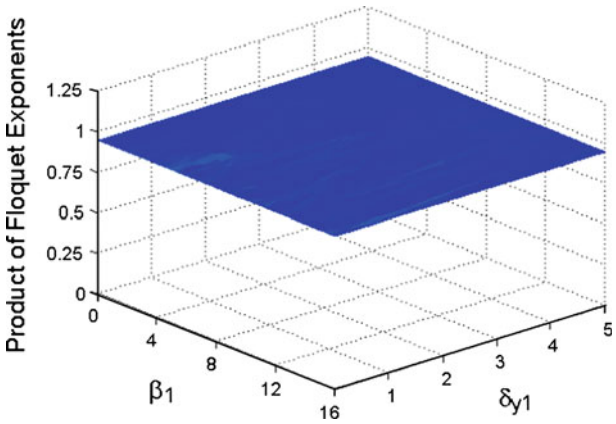

Fig. 8 Product of Floquet exponents for different values of δ_{y1} and β_1

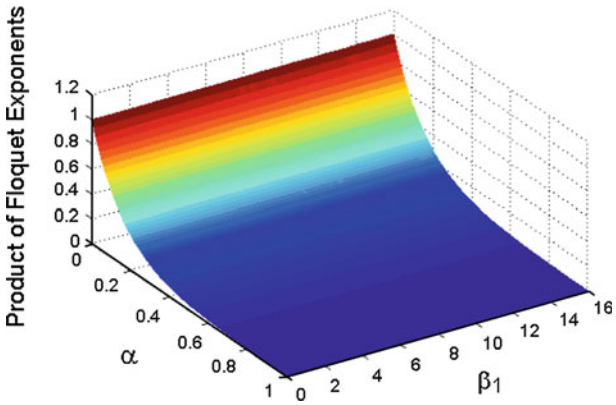

Fig. 9 Product of Floquet exponents for different values of β_1 and α

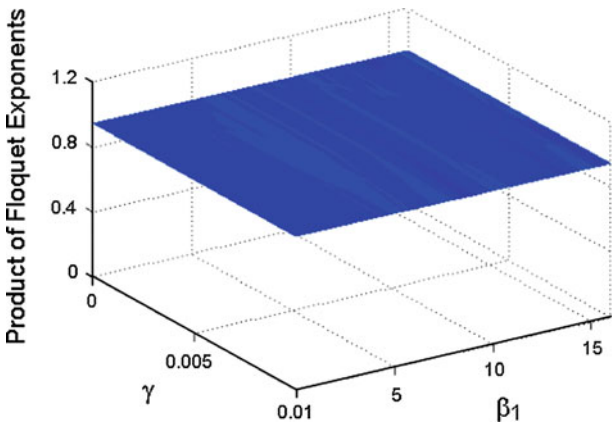

Fig. 10 Product of Floquet exponents for different values of β_1 and γ

The interesting point that the product of Floquet exponents reveals is that except the scaled damping α, other terms do not influence the contraction behavior of the response near the origin (see Figs. 8, 9 and 10). According to these Figures, even when the origin is unstable and the system response expands in the direction of the eigenvector corresponding to maximum Floquet exponent, the total behavior is in the form of contraction. It means that the trajectories of the system are attracted by another attracting set that is the stabilized periodic orbit in this case. By way of illustration, consider the first set of parameter values in Table 2. For this system, the eigenvalues and corresponding eigenvectors are presented in Table 3. As can be observed, in the drive mode (corresponding to the first two columns in the left side of Table 3), there is an expanding term in one

Table 3 Floquet exponents and corresponding eigenvectors of the linear system for the mentioned gyroscope

Eigenvalue	−1.309	−0.740	−0.984	−0.984
Corresponding Eigenvector	$\begin{Bmatrix} -0.7065 \\ 0.7078 \\ -0.00130 \\ 0.00185 \end{Bmatrix}$	$\begin{Bmatrix} 0.7107 \\ 0.7035 \\ -0.00132 \\ -0.00184 \end{Bmatrix}$	$\begin{Bmatrix} 0.0000 \\ 0.0012 \\ 1.000 \\ 0.0044 \end{Bmatrix}$	$\begin{Bmatrix} 0.0000 \\ 0.0011 \\ 0.0046 \\ 1.000 \end{Bmatrix}$

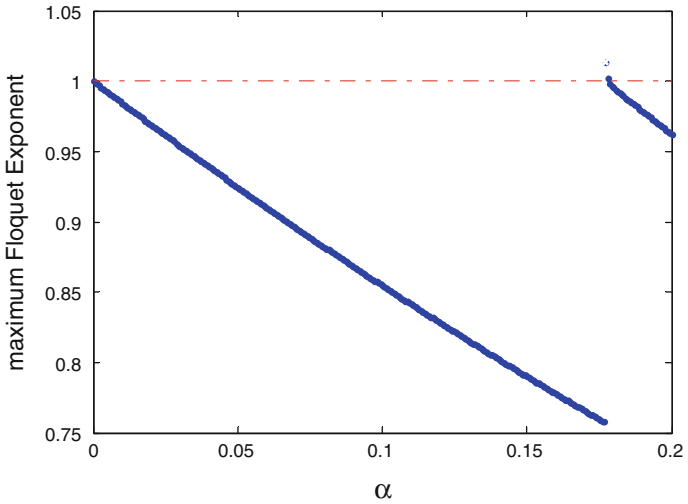

Fig. 11 Effect of α on the stability of periodic orbits

direction (by a factor of 1.309) and a contraction term in another direction (by 0.74). In the sense mode, the response in both directions is contracting, and the system expansion (contraction) factor in this case is 0.938.

6.2 Stability of periodic orbits of the nonlinear system

As previously discussed, stability of the periodic orbits of the considered gyroscope in Eq. (19) is evaluated by Floquet multipliers. According to the Floquet theory, the matrix $D(\tau)$ that governs the dynamics of perturbation is derived in Eq. (25):

$$D(\tau) = \left.\frac{\partial F}{\partial x}\right|_{x=x_r(\tau)} = \left[\begin{array}{cccc} 0 & 1 & 0 & 0 \\ -(\delta_x + 2\beta_x \cos 2\tau) - 3(\delta_{x3} + 2\beta_{x3}\cos 2\tau)\, x_1^2 & -\alpha_x & 0 & \gamma \\ 0 & 0 & 0 & 1 \\ 0 & -\gamma & -\delta_y - 3\delta_{y3}x_3^2 & -\alpha_y \end{array}\right]\Bigg|_{x=x_r(\tau)} . \quad (25)$$

As can be seen in Eq. (25), in order to compute Floquet exponents for periodic orbits, the time trend of the periodic orbit is required. The advantage of Floquet theory is that a numerical solution for the periodic orbit is adequate. A thorough study on methods of finding periodic orbits for the considered system is beyond the scope of this research and will be reported in another paper studying the bifurcations in the system. However, it should be mentioned that for small values of β_3, two stable periodic orbits with period 2π are dominant, which are identical to each other except for a π radian phase difference. As a consequence, one can rely on the steady state response of the gyroscope as its periodic orbit and study the effect of each parameter value on the stability of this orbit. There is only one thing that should be considered while using steady state response as the periodic orbit of the system: Since the trivial solution is the steady state response of the system when the origin is stable, while using the steady response as the periodic orbit, the corresponding Floquet exponents should be interpreted correctly as an indication of stability of the origin and not the periodic orbit.

Based on the discussed method, the effect of scaled damping α is studied in Fig. 11.

As expected, Fig. 11 shows that increasing α increases the stability of the periodic orbit by decreasing the maximum Floquet exponent. An interesting point about Fig. 11 is that when the origin becomes stable

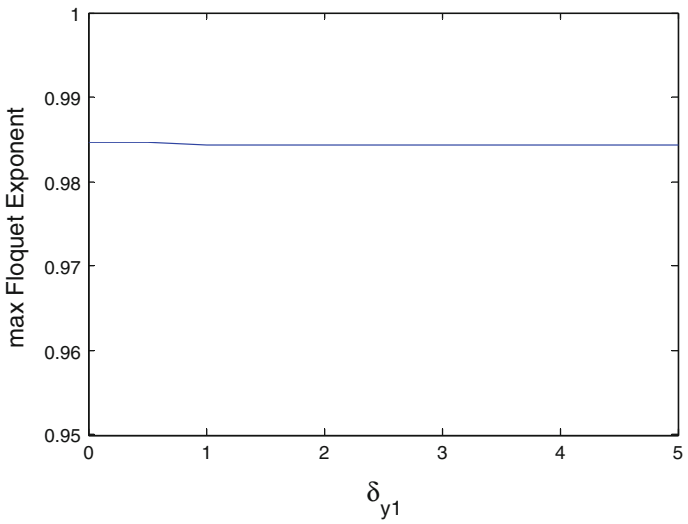

Fig. 12 Effect of δ_{y1} on the stability of periodic orbits

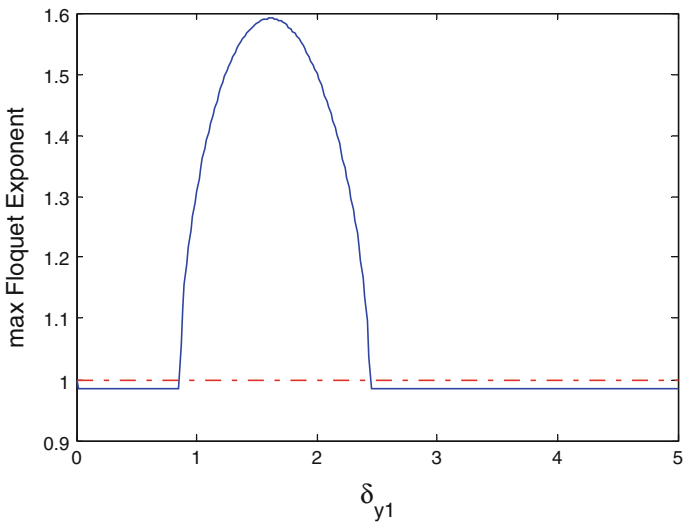

Fig. 13 Effect of δ_{y1} on the stability of the periodic origin

(the right-hand side of the figure), although the periodic orbits have stronger stability characteristics compared to the origin, these orbits are not the dominant attractors of the response of the gyroscope, and the solutions converge to the zero state.

The effect of δ_{y1} on the stability of the periodic orbit is illustrated in Fig. 12. Comparing Fig. 12 with the stability of the origin (Fig. 13) shows that although stability of the origin changes while δ_{y1} is changed, the stability of the periodic orbit is independent of changes in δ_{y1}. Another interesting point in Fig. 12 is that the dominant zero response is not due to instability of periodic orbits, but it is due to the stability of the origin. This conclusion was made because no change in the stability of periodic orbit occurs when zero response is obtained.

The effect of β_1 on the stability of the periodic orbit is shown in Fig. 14, and its effect the stability of the origin is presented in Fig. 15. Again, it can be concluded that β_1 has no effect on the stability of the periodic orbit, and also it can be concluded that the zero response is obtained whenever the origin becomes stable while the periodic orbits are still stable.

The remaining linear term γ (the scaled rotation rate) has no effect on the stability of periodic orbits in the operational range considered for it and hence, it is not shown here.

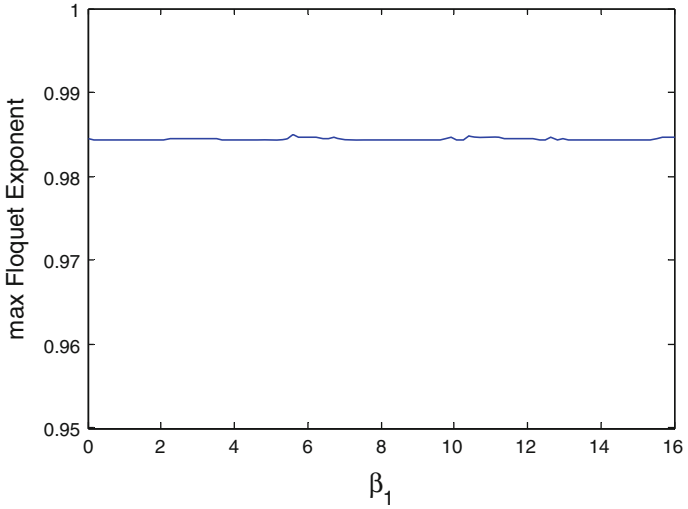

Fig. 14 Effect of β_1 on the stability of periodic orbits

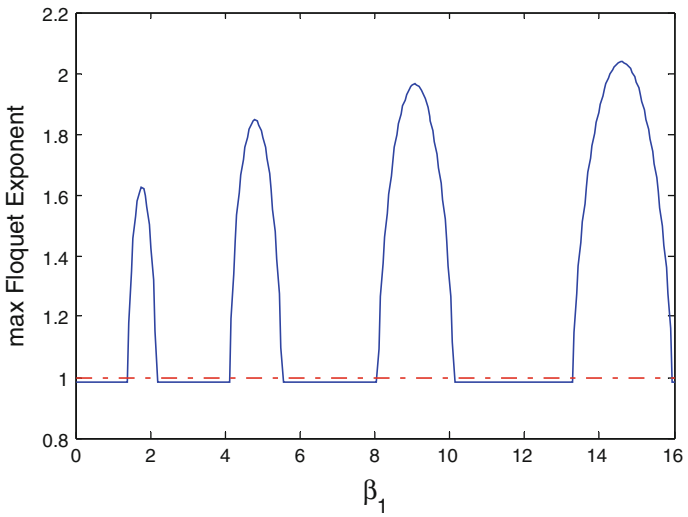

Fig. 15 Effect of β_1 on the stability of the periodic origin

Among the nonlinear terms δ_{x3}, δ_{y3} and β_3 (which are only two independent parameters since $\delta_{x3} = \delta_{y3} + 2\beta_3$ holds), δ_{y3} has only a scaling effect on the response and consequently does not affect the stability. By contrast, β_3 is the key parameter in bifurcations happening in the system. A thorough study on bifurcations related to β_3 will be discussed in another paper by the authors. Mentioned here, however, is that in order to have stable resonant-based high-amplitude periodic orbits for the gyroscope, β_3 should be kept as small in magnitude as possible in the interval $(-0.5, 0)$. While for other values of β_3 there are still resonant periodic orbits, due to the problems associated with the presence of other non-resonant periodic orbits, the operation of the gyroscope faces some fundamental difficulties and hence, these values should be avoided for β_3 [21].

7 Conclusion

In this paper, stabilities related to a parametrically resonated MEMS gyroscope are studied. These stabilities include those of the origin and of periodic orbits. The importance of studying the stability of the origin is that unlike harmonic excitation for which there is no stationary point, for parametric excitation the origin is always an equilibrium point. Hence, when the origin is asymptotically stable, the system response tends to a zero state rather than a periodic orbit.

For stability analysis, Floquet theory is implemented because it provides a simple numerical tool that quantitatively shows stability characteristics. Since Floquet theory is exclusively developed for studying periodic orbits and not for a stationary point, two propositions were developed to make Floquet theory applicable for the purpose of studying the stability of the origin.

As the study shows, the same parameters that influence the stability of the origin contribute to parametric resonance in the drive mode. Among these parameters, the value of the scaled stiffness δ_{y1} is the most important factor not for its relationship to stability issues but for its role in resonance in the sense mode. The linear parametric excitation factor β_1 has the key role in the instability of the origin and consequently in the occurrence of parametric resonance in the drive mode. The effect of the scaled damping coefficient α is that it increases stability of both the origin and the periodic orbit. However, large values of α make the origin stable and drop parametric resonance in the system. Since for operational purposes, the scaled rotation rate γ should be kept small, it cannot influence stabilities in the system.

The stability of periodic orbits is only influenced by the scaled damping α. Neither the linear terms (i.e., the scaled linear stiffness δ_{y1}, the parametric excitation factor β_1, the scaled product of the excitation voltage and the linear shape factor of the comb fingers, and the scaled rotation rate γ) nor the nonlinear terms (i.e., the scaled nonlinear stiffness δ_{y3} and the nonlinear parametric excitation factor β_3) can influence the stability of the periodic orbits. In fact, it can be shown that bifurcations due to β_3 occur while stabilities of periodic orbits are unchanged [21], and as a result, bifurcations are in the form of emergence of new orbits in the presence of previous orbits. Note that the relative values of β_1 and β_3 are determined by the relative position of the actuating comb fingers, but their values can be adjusted via the excitation voltage (see Table 1). The interesting point is that dominancy of zero response in non-resonant regions of the system results from the stability of the origin. It should be noted that in these cases periodic orbits are still stable but the response moves toward the origin because of its exponential stability.

The impact of this study is its importance in the design procedure of a parametrically excited MEMS gyroscope. Knowing the effect of each parameter on the stabilities of the system, one can search for the optimum values for the parameters that result in the highest output amplitudes with consumption of minimal energy.

References

1. Yazdi, N., Ayazi, F., Najafi, K.: Micromachined inertial sensors. Proc. IEEE **86**, 1640–1658 (1998)
2. Liu, G., Wang, A., Jiang, T., Jiao, J., Jang, J.B.: A novel tuning fork vibratory microgyroscope with improved spring beams. In: Proceedings of the 3rd IEEE International Conference on Nano/Micro Engineered and Molecular Systems, NEMS 2008, pp. 257–260. Sanya (2008)
3. Alper, S.E., Akin, T.: A symmetric surface micromachined gyroscope with decoupled oscillation modes. In: Proceedings of the 11th International Conference on Solid-State Sensors and Actuators, pp. 456–459. Munich, Germany (2001)
4. Alper, S.E., Akin, T.: Symmetrical and decoupled nickel microgyroscope on insulating substrate. J. Sens. Actuators A Phys. **115**, 336–350 (2004)
5. Alper, S.E., Akin, T.: A single-crystal silicon symmetrical and decoupled MEMS gyroscope on an insulating substrate. J. Microelectromech. Syst. **14**, 707–717 (2005)
6. Jeong, C., Seok, S., Lee, B., Kim, H., Chun, K.: A study on resonant frequency and Q factor tunings for MEMS vibratory gyroscopes. J. Micromech. Microeng. **14**, 1530–1536 (2004)
7. Sung, W.T., Lee, J.Y., Lee, J.G., Kang, T.: Design and fabrication of an automatic mode controlled vibratory gyroscope. In: Proceedings of the 19th IEEE International Conference on Micro Electro Mechanical Systems, pp. 674–677. Istanbul (2006)
8. Sung, S., Sung, W.T., Kim, C., Yun, S., Lee, Y.J.: On the mode-matched control of MEMS vibratory gyroscope via phase-domain analysis and design. IEEE/ASME Trans. Mechatron. **14**, 446–455 (2009)
9. Sung, W.T., Sung, S., Lee, J.Y., Kang, T., Lee, Y.J., Lee, J.G.: Development of a lateral velocity-controlled MEMS vibratory gyroscope and its performance test. J. Micromech. Microeng. **18**, 055028 (2008)
10. Park, S., Horowitz, R.: Adaptive control for the conventional mode of operation of MEMS gyroscopes. J. Microelectromech. Syst. **12**, 101–108 (2003)
11. Park, S., Horowitz, R.: New adaptive mode of operation for MEMS gyroscopes. J. Dyn. Syst. Meas. Control Trans. ASME **126**, 800–810 (2004)
12. Park, S., Horowitz, R., Hong, S.K., Nam, Y.: Trajectory-switching algorithm for a MEMS gyroscope. IEEE Trans. Instrum. Meas. **56**, 2561–2569 (2007)
13. Park, S., Horowitz, R., Tan, C.W.: Dynamics and control of a MEMS angle measuring gyroscope. J. Sens. Actuators A Phys. **144**, 56–63 (2008)
14. Oropeza-Ramos, L.A., Turner, K.L.: Parametric resonance amplification in a MEMGyroscope. In: Proceedings of the Fourth IEEE Conference on Sensors, pp. 660–663. Irvine, CA (2005)
15. Oropeza-Ramos, L.A., Burgner, C.B., Turner, K.L.: Robust micro-rate sensor actuated by parametric resonance. J. Sens. Actuators A Phys. **152**, 80–87 (2009)
16. Oropeza-Ramos, L.A., Burgner, C.B., Turner, K.L.: Inherently robust micro gyroscope actuated by parametric resonance. In: Proceedings of the MEMS 2008, pp. 872–875, Tucson, AZ (2008)

17. Oropeza-Ramos, L., Burgner, C.B., Turner, K.L.: Using parametric resonance to improve micro gyrsocope robustness. In: Gusev, E. et al. (eds.) Advanced Materials and Technologies for Micro/Nano-Devices, Sensors and Actuators, NATO Science for Peace and Security Series B: Physics and Biophysics, 2010, Part 4, 2010, pp. 299–309 (2010)
18. Zhang, W., Baskaran, R., Turner, K.L.: Nonlinear behavior of a parametric resonance-based mass sensor. In: Proceedings of the ASME International Mechanical Engineering Congress and Exposition, pp. 121–125. New Orleans, LO (2002)
19. DeMartini, B.E., Rhoads, J.F., Turner, K.L., Shaw, S.W., Moehlis, J.: Linear and nonlinear tuning of parametrically excited MEMS oscillators. J. Microelectromech. Syst. **16**, 310–318 (2007)
20. Miller, N.J., Shaw, S.W., Oropeza-Ramos, L.A., Turner, K.L.: Analysis of a novel MEMS gyroscope actuated by parametric resonance. In: Proceedings of the ENOC 2008, Saint Petersburg, Russia (2008)
21. Pakniyat, A.: On the nonlinear dynamics and bifurcations in a new class of MEMS gyroscopes with parametric resonance. M.S. Thesis, School of Mechanical Engineering, Sharif University of Technology, Tehran, Iran (2010)
22. Pakniyat, A., Salarieh, H., Vossoughi, G., Alasty, A.: A modification on performance of MEMS gyroscopes by parametro-harmonic excitation. In: Proceedings of the ASME 2010, 10th Biennial Conference on Engineering Systems Design and Analysis (ESDA2010), Istanbul, Turkey (2010)
23. Argyris, J., Faust, G., Haase, M.: An Exploration of Chaos: an Introduction for Natural Scientists and Engineers, vol. VII, North-Holland, Amsterdam (1994)
24. Khalil, H.K.: Nonlinear Systems, 3rd edn. Prentice Hall, New Jersey (2002)